Journal of NeuroVirology, 11: 166–179, 2005

ISSN: 1355-0284 print / 1538-2443 online
DOI: 10.1080/13550280590922810

Taylor & Francis
Taylor & Francis Group

Up-regulation of astrocyte cyclooxygenase-2, CCAAT/enhancer-binding protein-homology protein, glucose-related protein 78, eukaryotic initiation factor 2α, and c-Jun N-terminal kinase by a neurovirulent murine retrovirus

Hun-Taek Kim,[1] Wenan Qiang,[2] Na Liu,[2] Virginia L Scofield,[2] Paul KY Wong,[2] and George Stoica[1]

[1]*Department of Pathobiology, Texas A&M University, College Station, Texas, USA;* [2]*Department of Carcinogenesis, University of Texas M. D. Anderson Cancer Center, Science Park, Research Division, Smithville, Texas, USA*

In susceptible strains of mice, infection with the mutant retrovirus MoMuLV-*ts*1 causes a neurodegeneration and immunodeficiency syndrome that resembles human immunodeficiency virus–acquired immunodeficiency syndrome (HIV-AIDS). In this study the authors show increased expression of cyclooxygenase-2 (COX-2) in the brainstem tissues of *ts*1-infected mice. Up-regulated central nervous system (CNS) levels of this enzyme are associated with HIV-associated dementia and other inflammatory and neurodegenerative diseases such as amyotrophic lateral sclerosis, Alzheimer's disease, and Parkinson's disease. In brainstem sections, the authors find that astrocytes surrounding spongiform lesions contain increased amounts of immunoreactive COX-2. COX-2 is also up-regulated in cultured *ts*1-infected cells from the C1 astrocytic cell line, which also show activation of c-Jun N-terminal kinase (JNK) pathway. Markers of endoplasmic reticulum (ER) stress, specifically the CCAAT/enhancer-binding protein-homology protein (CHOP), the glucose-related protein 78 (GRP78), and phosphorylated eukaryotic initiation factor 2α (eIF2α), were also up-regulated in *ts*1-infected C1 astrocytes. Up-regulation of COX-2 and the above ER signaling factors was reversed by treatment of the infected cells with curcumin which specifically inhibits the JNK/c-Jun pathway. These findings indicate that the JNK/c-Jun pathway is most likely responsible for COX-2 expression induced by *ts*1 in astrocytes, and that *ts*1 infection in astrocytes may lead to up-regulation of both inflammatory and ER stress pathways in the central nervous system. Because COX-2 inhibitors are now widely used to treat inflammatory conditions in animals and humans, this finding suggests that these drugs may be useful for therapeutic intervention in neurodegenerative syndromes as well. *Journal of NeuroVirology* (2005) **11,** 166–179.

Keywords: astrocytes; COX-2; ER stress; JNK; retrovirus

Introduction

Moloney murine leukemia virus-TB (MoMuLV) is a type C retrovirus that induces T-cell lymphomas in susceptible strains of mice at ~6 to 8 months of age after infection at birth (Yuen and Szurek, 1989). A single-point mutation in the envelope gene of its temperature-sensitive mutant *ts*1 confers upon the virus the ability to deplete T cells and motor neurons

Address correspondence to Dr. Paul K. Y. Wong, Department of Carcinogenesis, University of Texas M. D. Anderson Cancer Center, Smithville, TX 78957, USA. E-mail: pkwong@mdanderson.org

This work was supported by NIH grants MH71583 and NS43984 (to P.K.Y.W.), NIEHS Center Grant ES07784, and NCI Core Grant CA16672. The authors thank Vanessa Edwards and Kara Waters for their assistance in preparing the manuscript. The authors also thank Dr. William S. Lynn for critical comments on the manuscript.

Received 8 September 2004; revised 3 November 2004; accepted 4 November 2004.

in susceptible strains of mice by 6 weeks of age after infection at birth (Wong *et al*, 1989, 1991; Szurek *et al*, 1990). Infection of the central nervous system (CNS) with *ts*1 causes a progressive neurodegenerative disease whose characteristic pathology includes spongiform degeneration and neuronal loss (Stoica *et al*, 1993, 2000). This neuronal loss is the most intriguing result of *ts*1 infection, because neurons themselves are not infected, but endothelial cells, microglia, oligodendrocytes, and astrocytes are. Thus, the neuronal loss in the infected mouse is most likely due to an inflammatory response by the infected glia and its secondary effects.

In diseases such as multiple sclerosis, amyotrophic lateral sclerosis (Almer *et al*, 2002; Mingetti, 2004), Alzheimer's disease (Pasinetti and Aisen 1998), Parkinson's disease (Teismann *et al*, 2003), and human immunodeficiency virus (HIV)-associated dementia (Kusdra *et al*, 2002), brain tissues contain high levels of cyclooxygenase (COX)-2, a potent activator of inflammation, and of its biosynthetic product prostaglandin (PG)E_2. In all of these diseases, astrocytes and microglia are the major sources of COX-2 and PGE_2 (Mingetti *et al*, 1999; Molina-Holgado *et al*, 2000). Virus infections in general tend to stimulate COX-2 expression (Murono *et al*, 2001; Janelle *et al*, 2002; Seymour *et al*, 2002), and inhibitors of COX-2 activity attenuate virus replication (Chen *et al*, 2000; Zhu *et al*, 2002), suggesting that COX-2 activation and the cellular events that follow are important determinants governing viral replication and the spread of infection and cellular damage in the CNS.

At this time, several COX-2 inhibitors are available over the counter for treatment of inflammatory conditions outside the CNS. No prior studies have investigated inhibitors of COX-2 expression as potential therapies following virus infection of glial cells in the brain. To make this connection, the relevant COX-2 regulatory pathway must be identified in at least one of the relevant cell types (i.e., astrocytes), because transcriptional regulation of COX-2 expression occurs by multiple signal transduction pathways, and differs by cell type (Subbaramaiah *et al*, 1996; Newton *et al*, 1997; Tai *et al*, 1997; Reddy *et al*, 2000; Slice *et al*, 2000; Wadleigh *et al*, 2000). The three signal transduction pathways known to up-regulate COX-2 all involve members of the mitogen-activated protein kinase (MAPK) superfamily, and include (a) extracellur regular kinase (ERK) (Subbaramaiah *et al*, 1998; LaPointe and Isenovic, 1999), (b) c-Jun N-terminal kinase (JNK) (Xie and Herschman, 1996; Guan *et al*, 1998; Subbaramaiah *et al*, 1998), and (c) p38 (LaPointe and Isenovic, 1999; Laporte *et al*, 2000).

In cultured *ts*1-infected primary astrocytes and cells of the *ts*1-infected C1 astrocytic cell line, viral envelope precursor proteins accumulate in the endoplasmic reticulum (ER) (Shikova *et al*, 1993; Lin *et al*, 1997) and trigger an ER stress response, resulting in increased reactive oxygen species (ROS) production (Liu *et al*, 2004; Qiang *et al*, 2004) with activation of nuclear factor (NF)κB which stimulates the expression of inducible nitric oxide synthases (iNOS) (Kim *et al*, 2001) and the production of proinflammatory cytokines (Choe *et al*, 1998). In general, ER stress involves two signal transduction pathways, which are the ER overload response, or EOR, and the unfolded protein response, or UPR (Kozutsumi *et al*, 1988; Pahl and Baeuerle, 1996). In the UPR, the ER transmembrane kinases IRE1 (inositol-requiring enzyme-1) and PERK (double-stranded RNA-dependent protein kinase [PKR]-like ER kinase) are activated. ROS overproduction in *ts*1-infected astrocytes additionally activates a cellular antioxidant response via the transcription factor Nrf-2, to activate the biosynthetic machinery for production and maintenance of protective intracellular thiols (Qiang *et al*, 2004). In this study, we show that *ts*1 infection induces COX-2 expression in the brainstems of infected mice and in cultured cells of the C1 astrocytic cell line. In these cells, *ts*1 infection specifically activates the JNK/c-Jun signaling pathway, together with ER stress signaling. Both of these intracellular cascades can be blocked by treatment with the JNK inhibitor curcumin. Together these results suggest that *ts*1-induced oxidative stress and inflammatory responses in astrocytes may be responsible for neuronal loss and neurodegeneration in the *ts*1-infected brain. The data also suggest that COX-2 inhibitors and nontoxic nutrient antioxidants (e.g., curcumin) may be effective treatments for this and other neurodegenerative diseases.

Results

Increased expression of COX-2 mRNA and protein in the brainstems of ts1-infected mice

To identify cell types in which COX-2 up-regulation occurs in the ts1-infected brainstem, we performed immunohistochemistry for COX-2 on sections from CNS tissues of control uninfected versus *ts*1-infected mice. Figure 1a shows that astrocytes in sections from an uninfected brainstem showed no binding by the anti-COX-2 antibody, whereas Figure 1b shows that cells in *ts*1-infected brainstems displayed moderate-to-strong cytoplasmic immunostaining in cells having clear astrocytic morphology.

To determine whether *ts*1 infection induces COX-2 gene expression in the CNS of infected mice, semiquantitative reverse transcriptase–polymerase chain reaction (RT-PCR) was used to measure the expression of COX-2 mRNAs in brainstems of control and *ts*1-infected animals at 25 days post infection (dpi). Figure 1c and Figure 1d show that COX-2 mRNA levels were four times higher in brainstem tissues of *ts*1-infected mice than in brainstem tissues from uninfected control mice. Figure 1e and Figure 1f show that amounts of COX-2 protein in brainstem homogenates of *ts*1-infected mice were also significantly higher in

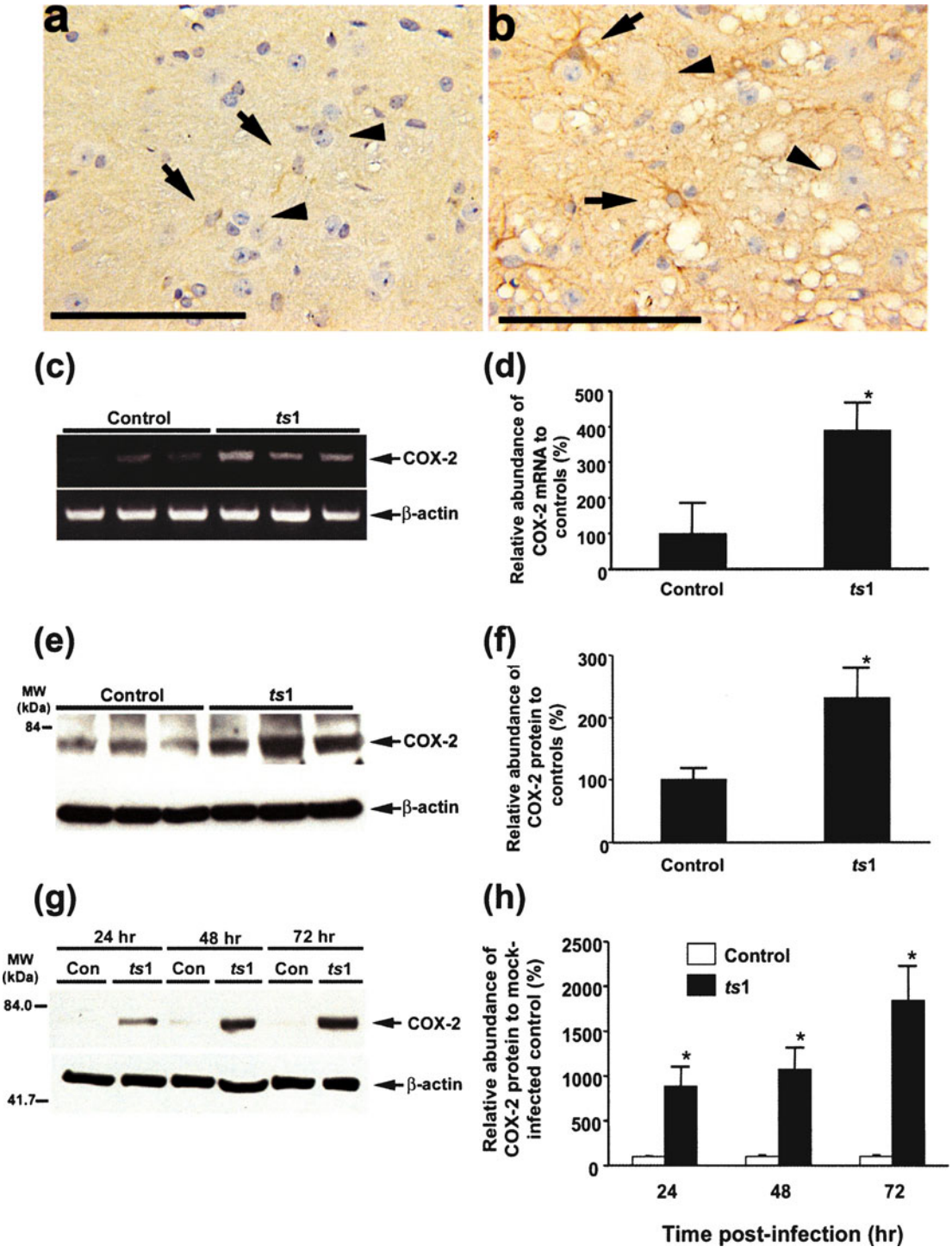

Figure 1 Expression of COX-2 protein in the brainstems of control versus *ts*1-infected mice, and in *ts*1-infected astrocytic cells. (**a**) COX-2 immunoreactivity (*brown*) in the cytoplasm of brainstem astrocytes from a control mouse. Astrocytes were identified by their characteristic stellate morphology and long processes. Note the absent or weak cytoplasmic staining for COX-2 in astrocytes (*arrows*) and neurons (*arrowheads*). (**b**) COX-2 immunoreactivity in the cytoplasm of astrocytes in *ts*1-infected brainstem tissue. Strong COX-2 staining is present in astrocytes (*arrows*) but absent in neurons (*arrowheads*). (**c**) Semiquantitative RT-PCR analysis of COX-2 mRNA in total RNAs from brainstems of control and *ts*1-infected mice at 25 dpi. (**d**) Comparison of COX-2 mRNA levels in brainstems of *ts*1-infected versus control mice. (**e**) Western blot showing levels of COX-2 protein in brainstems of *ts*1-infected mice versus controls at 25 dpi. MW = molecular weight in kilodaltons (kDa). (**f**) Densitometric analysis of COX-2 protein bands in brainstems of control versus *ts*1-infected mice. The results shown in the histograms are the mean ± standard deviation (SD) for tissues from three control and three *ts*1-infected mice. *Significantly different from mock-infected controls ($P < .01$). (**g**) Western blot showing COX-2 protein levels in control and *ts*1-infected C1 cells at 24, 48, and 72 h post infection (pi) (*top*). (**h**) Densitometric quantitation of COX-2 protein in mock-infected versus *ts*1-infected C1 cells at 24, 48, and 72 h pi. The results for each time point are the mean ± SD from three independent experiments. Con = mock-infected cells; *ts*1 = *ts*1-infected cells. *Significantly different from mock-infected controls ($P < .01$).

*ts*1-infected brainstem tissues, relative to control tissues, at 25 dpi ($P < .01$).

Increased expression of COX-2 in cultured astrocytes infected with ts*1*

Cells of the immortalized astrocyte cell line C1 resemble primary astrocytes in their stellate morphology and in their expression of the astrocyte-specific marker glial fibrillar acidic protein (GFAP) (Lin *et al*, 1997). It has also been reported that C1 astrocytes and primary astrocytes share common characteristics in their response to *ts*1 infection, and that findings from these immortalized astrocytes are applicable to primary cultures (Liu *et al*, 2004; Qiang *et al*, 2004). As C1 cells are more readily available for experimentation, we asked whether the increased COX-2 expression seen in *ts*1-infected mice is also increased in C1 cells infected with by *ts*1. Figure 1g and Figure 1h show that amounts of COX-2 protein were significantly elevated in *ts*1-infected C1 cells, relative to mock-infected cells, at 24, 48, and 72 h post infection ($P < .01$). In addition, COX-2 protein was elevated in *ts*1-infected primary cultured astrocytes (data not shown). The signal transduction pathways involved in the induction of COX-2 expression in these cells by *ts*1 infection were then evaluated.

The JNK/c-Jun signal transduction pathway governs COX-2 up-regulation in ts*1-infected C1 cells*

COX-2 gene expression requires the activation of at least one of three known MAPK pathways (Guan *et al*, 1998; Newton *et al*, 2000; Wadleigh *et al*, 2000; Kyriakis and Avruch, 2001). To determine which of these participates in COX-2 up-regulation after *ts*1 infection of astrocytic cells, we used Western blotting to compare amounts of these three MAPKs in *ts*1-infected versus control C1 cells over time after infection (at 24, 48, and 72 h pi). Figure 2a, 2b, and 2c show that both phosphorylated JNK proteins and phosphorylated ERK1/2 proteins increased in a time-dependent manner in the infected cells, whereas p38 phosphorylation was not significantly until 72 h pi (Figure 2a and 2d). These results show that both the JNK and ERK1/2 MAPK are phosphorylated in association with increased COX-2 expression in *ts*1-infected C1 cells.

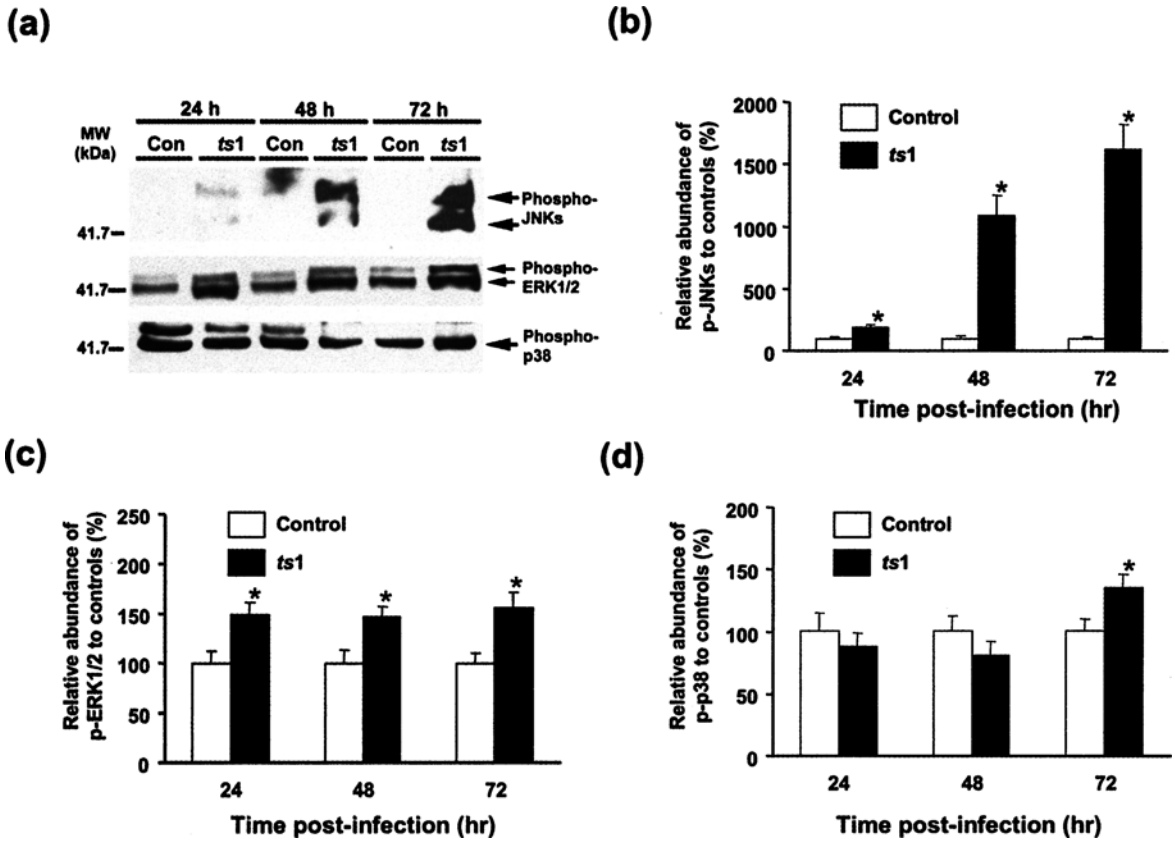

Figure 2 Specific phosphorylation of the JNKs/c-Jun MAPK enzyme in *ts*1-infected C1 cells. C1 astrocytes were either mock-infected or infected with *ts*1, followed by culturing and preparation of whole cell lysates at 24, 48, and 72 h pi. (**a**) Western blot showing levels of three different phosphorylated MAPKs in control and *ts*1-infected C1 astrocytes at 24, 48, and 72 h pi. (**b**, **c**, and **d**) Phosphorylated JNKs, phosphorylated ERKs (p-ERK1/2), and phosphorylated p38 (p-p38) in mock-infected versus *ts*1-infected C1 astrocytes. Con = mock-infected cells; *ts*1 = *ts*1-infected cells. The results are the mean ± SD from three independent experiments, each run in duplicate. *Significantly different from mock-infected controls ($P < .01$).

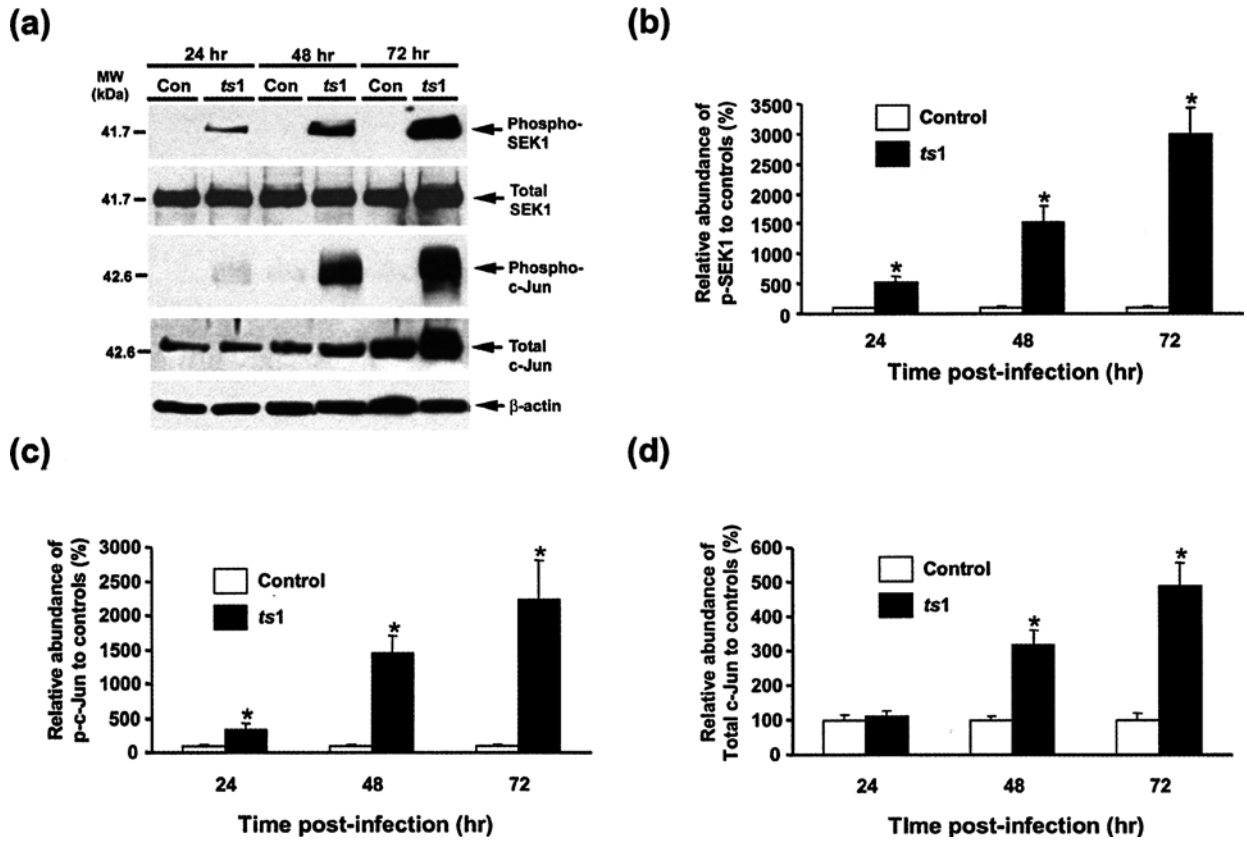

Figure 3 Effect of *ts*1 infection on levels of phosphorylated SEK1, phosphorylated c-Jun, total SEK1, and total c-Jun proteins. C1 astrocytes were mock-infected or infected with *ts*1, and whole-cell lysates prepared at 24, 48, and 72 h pi. (**a**) Western blot showing levels of phosphorylated SEK1, total SEK1, phosphorylated c-Jun, and total c-Jun proteins in control and *ts*1-infected C1 astrocytes. (**b**,**c**, and **d**) Phosphorylated SEK1 (p-SEK1), phosphorylated c-Jun (p-c-Jun), and total c-Jun in mock-infected versus *ts*1-infected C1 astrocytes. The results are the mean ± SD from three independent experiments, each run in duplicate. Con = mock-infected cells; *ts*1 = *ts*1-infected cells. *Significantly different from mock-infected controls ($P < .01$).

To confirm the involvement of the JNK/c-Jun pathway in COX-2 expression in *ts*1-infected C1 cells, we measured levels of upstream and downstream intermediates in this pathway in control and *ts*1-infected cells over time. To determine whether JNK phosphorylation is mediated through its upstream activator stress-activated protein kinase/ERK kinase (SEK1), and to ascertain whether phosphorylated JNK phosphorylates its downstream substrate c-Jun, we measured levels of phosphorylated SEK1 and c-Jun proteins in *ts*1-infected and mock-infected C1 cells, again at 24, 48, and 72 hr pi. Figure 3 shows that levels of phosphorylated SEK1, phosphorylated c-Jun, and total c-Jun were increased over time after infection of C1 cells with *ts*1. The patterns of expression of these substrates, together with the timecourse of phosphorylated JNK increase shown in Figure 2a and 2b, suggest that activation of the JNK/c-Jun pathway increases COX-2 expression after *ts*1 infection in C1 astrocytes.

JNK pathway inhibitors prevent COX-2 up-regulation in ts*1-infected C1 cells*

To further confirm that JNK is required for COX-2 up-regulation after *ts*1 infection of astrocytic cells, and to explore the possibility that ERK1/2 is also required (as suggested by data in Figure 2a and 2c), C1 cells were treated with curcumin and SP600125, both of which are JNK pathway inhibitors (Hanazawa *et al*, 1993; Mohan *et al*, 2000; Seol *et al*, 2000; Bennett *et al*, 2001). Figure 4 shows that both agents decreased levels of COX-2, phosphorylated JNKs, and phosphorylated c-Jun in a dose-dependent manner. Notably, however, neither agent decreased levels of phosphorylated ERK1/2 or p38 proteins in *ts*1-infected C1 cells (data not shown). These results argue against the idea that the ERK1/2-MAPK pathway is a primary participant in the signal transduction events leading to up-regulation of COX-2 expression in *ts*1-infected C1 cells. However, we performed one more experiment to confirm that ERK1/2 are secondary to JNKs in the cellular events associated with COX-2 elevation in these cells.

PD98059 (used at 10 μM) is a selective inhibitor of mitogen-activated protein kinase (MEK), an upstream regulator of ERKs (Alessi *et al*, 1995). When PD98059 was added to *ts*1-infected C1 cultures, the levels of phosphorylated ERK1/2 were significantly decreased (Figure 5a and 5b; $P < .01$), although increases in COX-2 levels still occurred (Figure 5a and

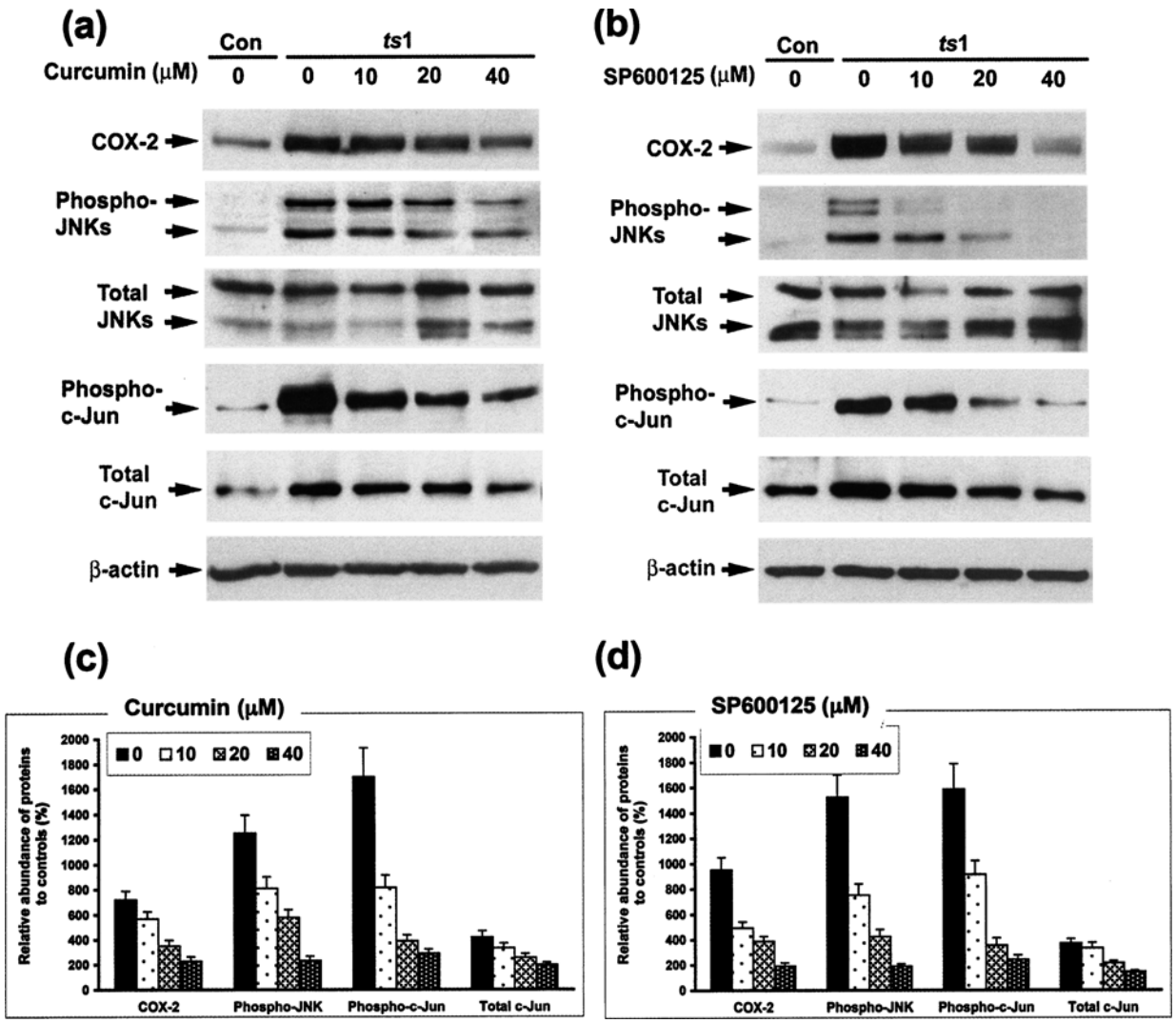

Figure 4 Effects of the JNK inhibitors curcumin or SP600125 on levels of COX-2 in *ts*1-infected astrocytes. C1 astrocytes were either mock-infected or infected with *ts*1, and whole cell lysates were prepared at 48 h pi after incubation for 16 h with varying concentrations of curcumin (10, 20, and 40 μM) and SP600125 (10, 20, and 40 μM). (**a**) Western blot showing COX-2, phosphorylated JNKs, total JNKs, phosphorylated c-Jun, and total c-Jun proteins in control versus *ts*1-infected C1 cells either left untreated or treated with curcumin. (**b**) Western blot showing COX-2, phosphorylated JNKs, phosphorylated c-Jun, and total c-Jun proteins in *ts*1-infected C1 cells treated with SP600125. (**c** and **d**) Densitometric quantitation of protein bands in (**a**) and (**b**). Data in (**c**) and (**d**) are presented as percentage increases in amounts of proteins in treated versus untreated *ts*1-infected cells relative to levels for mock-infected control cells treated with DMSO. Results are expressed as the mean ± SD from three independent experiments, each run in duplicate.

5b). Together, these results are consistent with our other data indicating that the JNK pathway, not the ERK1/2 pathway, specifically regulates COX-2 expression in *ts*1-infected astrocytes.

Proteasome inhibitors increase COX-2 via JNK and p38 MAPK-dependent pathways, but not ERK1/2-dependent pathways

Given the involvement of JNKs in *ts*1-mediated activation of COX-2, and given the ability of proteasome inhibitors to activate JNK pathways (Kaufman, 1999; Nishitoh *et al*, 2002), we tested whether proteasome inhibitors would amplify *ts*1-mediated JNK activation and COX-2 expression. Figure 6a shows that treatment of C1 cells with the proteasome inhibitor MG-132 resulted in further increases in amounts of COX-2 in *ts*1-infected cells, relative to the effects of infection alone, whereas calpeptin, a selective inhibitor of the calpain proteolytic pathway (which is independent of proteasome activation; Jiang *et al*, 1996), did not increase production of COX-2. Figure 6a also shows that MG-132 treatment elevated amounts of phospho-JNKs, phospho-SEK1, and phospho-c-Jun in *ts*1-infected C1 cells.

We also tested two other proteasome inhibitors (ALLN and lactacystin), both known to elevate levels of phosphorylated JNK, phosphorylated p38 MAPK, and COX-2, and found that they also increase amounts of phospho-JNKs, together with COX-2, in *ts*1-infected C1 cells (Figure 6b). Notably, these

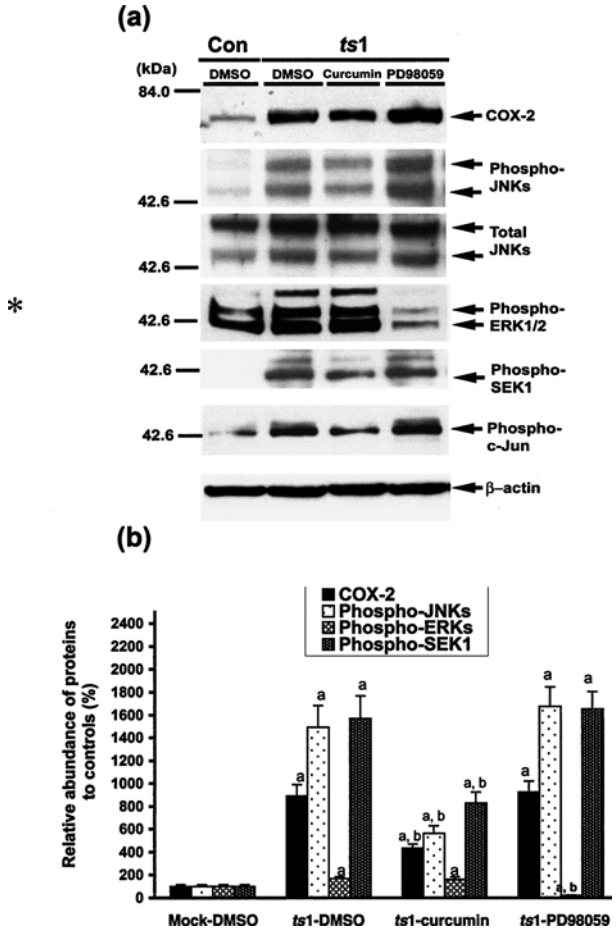

Figure 5 Effects of curcumin and PD98059 on levels of COX-2, phosphorylated JNKs, phosphorylated ERKs, and phosphorylated SEK1 in *ts*1-infected astrocytes. C1 astrocytes were either mock-infected or infected (DMSO alone) with *ts*1, and whole-cell lysates were prepared at 48 h pi after incubation for 16 h with curcumin (20 μM) or PD98059 (10 μM). (**a**) Western blot showing COX-2, phosphorylated JNKs, phosphorylated ERK1/2, phosphorylated SEK1, and phosphorylated c-Jun proteins in uninfected versus *ts*1-infected C1 cells either left untreated or treated either with curcumin or with PD98059. (**b**) Densitometric comparison of COX-2, phosphorylated JNKs, phosphorylated ERK1/2, and phosphorylated SEK1 protein bands from (**a**). The results are the mean ± SD from three independent experiments, each run in duplicate. a = significantly different from mock-infected controls ($P < .01$). b = significantly different from *ts*1-infected untreated (DMSO-treated) control cells ($P < .01$).

two inhibitors decreased levels of phosphorylated ERK1/2 proteins and their downstream target p90 ribosomal S6 kinase (RSK) in infected C1 cells (Figure 6b). The summary Figure 6c shows densitometry tracings for COX-2 and phospho-JNK expression in the presence of all proteasome inhibitors tested and in the presence of calpeptin. In addition to confirming the central role played by the JNK and MAPK pathways in COX-2 up-regulation following *ts*1 infection of C1 cells, these data show that COX-2 up-regulation occurs under conditions in which the ERK1/2 signal transduction pathway is inhibited, further indicating that the ERK1/2 signal transduction pathway is not directly involved in this sequence of events.

Curcumin inhibits ER stress in ts1-infected C1 cells

Previous work from this laboratory has shown that *ts*1-induced cytopathic effects in primary astrocyte cultures are associated with accumulation of uncleaved *ts*1 envelope preprotein ($gPr80^{env}$)in the ER (Shikova *et al*, 1993). More recent work by Liu *et al* (2004) documents that *ts*1 infection of astrocytes activates ER stress signaling pathways, as detected by induction of CHOP, glucose-related protein 78 (GRP78), and phosphorylated eukaryotic initiation factor 2α (eIF2α) proteins, all of which are markers of the ER-PERK pathway. ER stress is known to activate the inositol-requiring enzyme 1 (IRE1)-SEK1/JNK pathway (Ron and Habener, 1992; Kaufman, 1999; Harding *et al*, 2000). Surprisingly, after curcumin treatment, the levels of these PERK marker proteins (CHOP, GRP78, and phosphorylated eIF2α) are reduced, whereas the ERK1/2-specific inhibitor PD98059 had no effect as shown in (Figure 7a and 7b). These data show that curcumin may reduce ER stress in *ts*1-infected C1 cells.

Discussion

Our laboratory has shown previoiusly that *ts*1 retrovirus–induced neurovirulence correlates with viral envelope precursor protein accumulation and ER stress in infected astrocytes (both primary and C1). This results in ROS, iNOS, and pro-inflammatory cytokine production, and in depletion of intracellular cysteine stores (Choe *et al*, 1998; Kim *et al*, 2001; Shikova *et al*, 1993; Liu *et al*, 2004; Qiang *et al*, 2004). It is now clear that oxidative stress plays an important role in the pathogenesis of various human and animal neurodegenerative diseases, such as Alzheimer's disease, Parkinson's disease, amyotrophic lateral sclerosis, and transmissible spongiform encephalitis. ROS signaling appears to be critical for the cellular inflammatory responses characteristic of these conditions, through the activation of redox-sensitive transcription factors and proinflammatory gene expression. Further understanding of the effects and roles of oxidative stress and inflammatory responses in these conditions will provide important insights regarding brain pathological processes contributing to neurodegeneration.

We show here that COX-2 expression is induced in the brainstems of *ts*1-infected mice and in *ts*1-infected C1 astrocytes, and we identify the JNK/c-Jun pathway as essential to this response. As shown in Figure 3, *ts*1-induced JNK activation is associated with an increase in the phosphorylation of the JNK-dependent transcription factor c-Jun. Because c-Jun phosphorylation enables formation of the activator protein (AP)-1 complex, *ts*1-induced JNK activation may up-regulate both COX-2 gene expression and

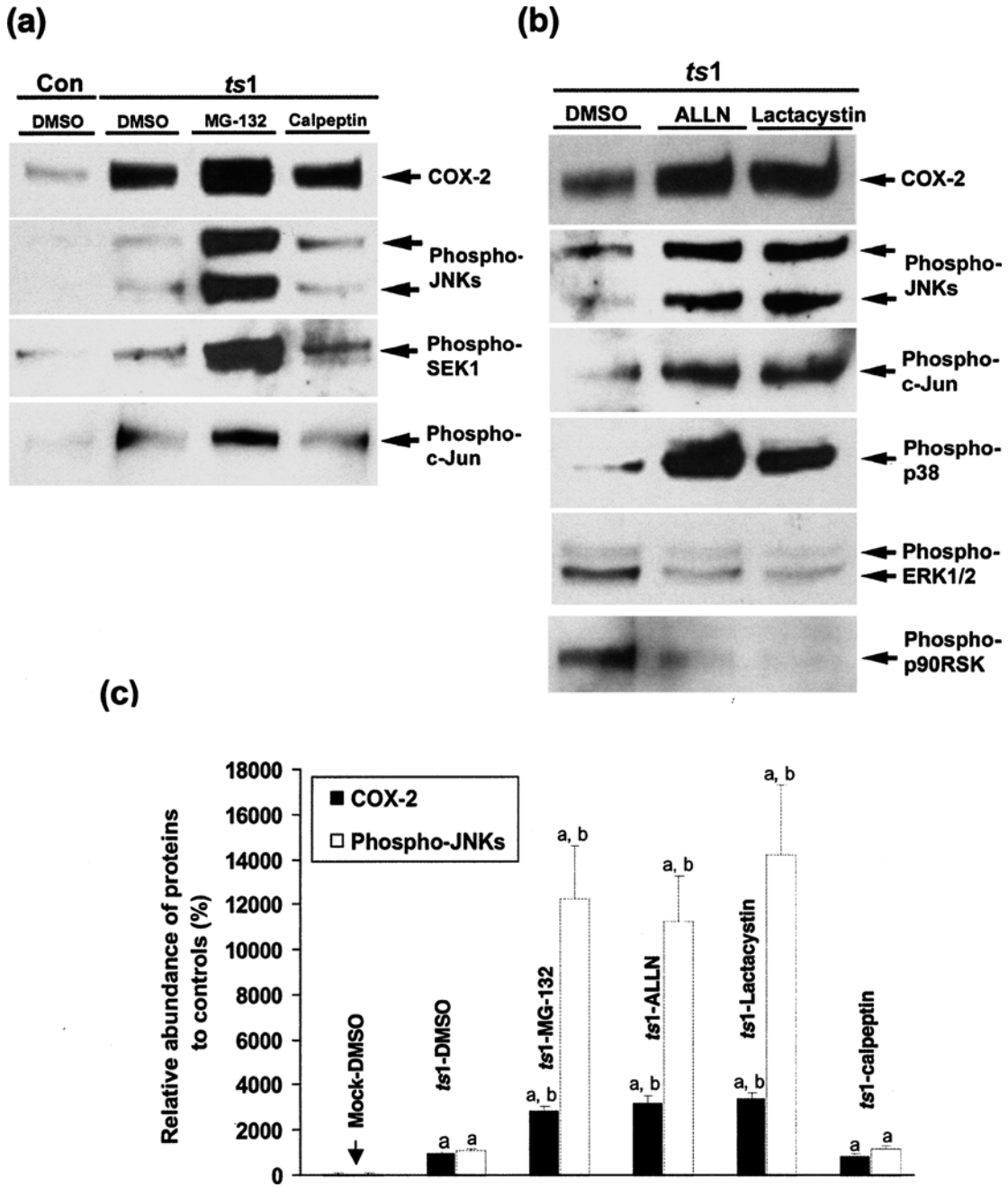

Figure 6 Effect of proteasome inhibitors on COX-2 expression and on phosphorylation of SEK1, JNK, p38, c-Jun, ERK1/2, and p90RSK in control versus *ts*1-infected C1 cells. C1 astrocytes were either mock-infected (DMSO alone) or infected with *ts*1, and whole-cell lysates were prepared 48 h pi after incubation for 16 h with MG132 (10 μM), calpeptin (10 μM), ALLN (5 μM), or lactacystin (10 μM). (**a**) Western blot showing levels of COX-2, phosphorylated JNKs, phosphorylated SEK1, and phosphorylated c-Jun proteins in uninfected versus *ts*1-infected C1 cells either left untreated (DMSO) or treated with MG-132 or calpeptin. (**b**) Western blot showing levels of COX-2, phosphorylated JNKs, phosphorylated c-Jun, phosphorylated p38, phosphorylated ERK1/2, and phosphorylated p90RSK in *ts*1-infected cells either left untreated (DMSO) or treated with ALLN or lactacystin. Similar results were obtained in two additional independent experiments. Con = mock-infected cells; *ts*1 = *ts*1-infected cells. (**c**) Densitometric analysis of protein bands in (**a**) and (**b**). The results are the mean ± SD from three independent experiments, each run in duplicate. a = significantly different from mock-infected controls ($P < .01$). b = significantly different from *ts*1-infected untreated (DMSO-treated) cells ($P < .01$).

c-Jun gene expression via cyclic adenosine monophosphate (cAMP)-responsive elements present in both promoters (Kitabayashi *et al*, 1990; Han *et al*, 1992; Herr *et al*, 1994). This idea is consistent with our previous observation that the activity of adenylate cyclase, the major activator of cAMP-dependent protein kinase, is altered in C1 cells infected with *ts*1 (Raofi *et al*, 2000). It is also consistent with our results, reported here, showing that amounts of total c-Jun are higher in *ts*1-infected C1 cells

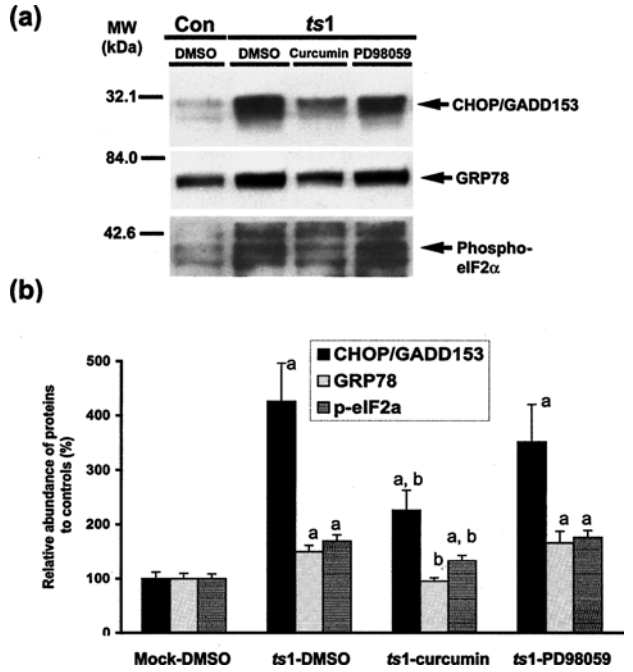

Figure 7 Curcumin, but not PD98059, inhibits *ts*1-induced up-regulation of CHOP and GRP78, and reduces levels of phosphorylated eIF2α. C1 cells were either mock infected or infected with *ts*1. At 24 h pi, the culture medium was exchanged for medium containing either 20 μM of curcumin or 10 μM of PD98059. After incubation in these drugs for 16 h, whole-cell lysates were prepared and analyzed by Western blotting. (**a**) Western blot showing levels of CHOP, GRP78, and phosphorylated eIF2α proteins in control C1 cells and *ts*1-infected C1 cells treated with curcumin or PD98059. (**b**) Densitometric comparison of CHOP/GADD153, GRP78, and phosphorylated eIF2α (p-eIF2α) protein bands in (**a**). Results are the means $\pm$ SD from two independent experiments carried out in triplicate ($n = 6$). Con = mock-infected cells; *ts*1 = *ts*1-infected cells. a = significantly different from mock-infected controls ($P < .01$). b = significantly different from *ts*1-infected control (DMSO-treated) cells ($P < .01$).

than in uninfected control cultures. Because total c-Jun levels increase over time in both control and the *ts*1-infected C1 cells (Figure 3a and 3d), basal expression of c-Jun may be independent of JNK activation, and may be regulated by another pathway.

Inhibition of proteasome function by specific inhibitors causes protein accumulation with ER stress responses (Nishitoh *et al*, 2002), as well as activation of the JNK and p38 MAPKs (Hanazawa *et al*, 1993; Merlin *et al*, 1998; Seol *et al*, 2000; Nakayama *et al*, 2001; Wu *et al*, 2002). In the work presented here, activation of JNK and p38 by proteasome inhibitors was associated with increased COX-2 expression in *ts*1-infected C1 cells (Figures 4 and 6). A specific p38 inhibitor, SB203580, reduced the up-regulated production of COX-2 in *ts*1-infected C1 astrocytes at 72 h post infection (results not shown), suggesting that p38 MAPK–dependent pathways may be involved in this event. However, p38 activity in *ts*1-infected C1 cells was similar to that of mock-infected cells at 24 and 48 h post infection, and only slightly higher than that of control cells at 72 h (Figure 2d), suggesting that although p38 may be involved, it may not be rate-limiting for COX-2 expression in infected astrocytes.

What are the mechanisms responsible for activation of the SEK1/JNK/c-Jun pathway in *ts*1-infected cells? Work by ourselves and others has shown that neurovirulent virus and prion infection can cause ER stress in infected cells (Shikova *et al*, 1993; Su *et al*, 2002; Dimcheff *et al*, 2003; Liu *et al*, 2004). IRE1 activates the downstream mediators SEK1 and JNK (Tirasophon *et al*, 1998; Kaufman, 1999; Urano *et al*, 2000; Iwawaki *et al*, 2001; Nishitoh *et al*, 2002). In the present study, therefore, the upstream kinase responsible for SEK1/JNK and COX-2 activation in astrocytes by *ts*1 infection is likely to be IRE1 (Figure 8).

Work by others has also shown that curcumin suppresses JNK activation by blocking signals from upstream kinases without directly inhibiting either JNK or SEK1 (Chen and Tan, 1998; Jobin *et al*, 1999). A particularly interesting observation from the present study is that although SP600125 did not affect levels of the PERK pathway markers CHOP, GRP78, and phosphorylated eIF2α (results not shown), curcumin treatment inhibited these ER stress signaling pathways (Figure 4a and 4c). These results suggest that curcumin may suppress ER stress signaling through targets upstream of IRE1 and PERK. Notably, curcumin has been shown to have antioxidant activity (Sharma, 1976; Scapagnini *et al*, 2002), and we have shown that *ts*1-induced ER stress causes oxidative stress, and that this in turn can amplify ER stress (Liu *et al*, 2002, 2004; Qiang *et al*, 2004). It seems likely, in light of this information, that curcumin dampens ER stress by inhibiting oxidative stress. At present, the way in which curcumin might exert this effect remains to be determined.

To our knowledge, this is the first report of a role for ER stress in the up-regulation of COX-2 by retrovirus infection, both *in vivo* and *in vitro*. The results of the present study add to our previous findings linking *ts*1 infection of astrocytes to an ER stress response that (a) activates SEK1/JNK/c-Jun signaling pathways, and (b) elevates COX-2 production. A schematic representation of possible pathways involved in this sequence appears in Figure 8.

The data presented here also imply that the inflammatory consequences of *ts*1 infection in astrocytes (reflected by COX-2 up-regulation) are direct consequences of ER stress responses activated in these cells after infection by *ts*1 (following JNK phosphorylation). Our results have identified the JNK intracellular signaling pathway as the primary cause of ER stress in retrovirus-infected astrocytes. The data also identify COX-2 and its regulatory pathways as potential targets for therapeutic intervention in neurodegenerative disease.

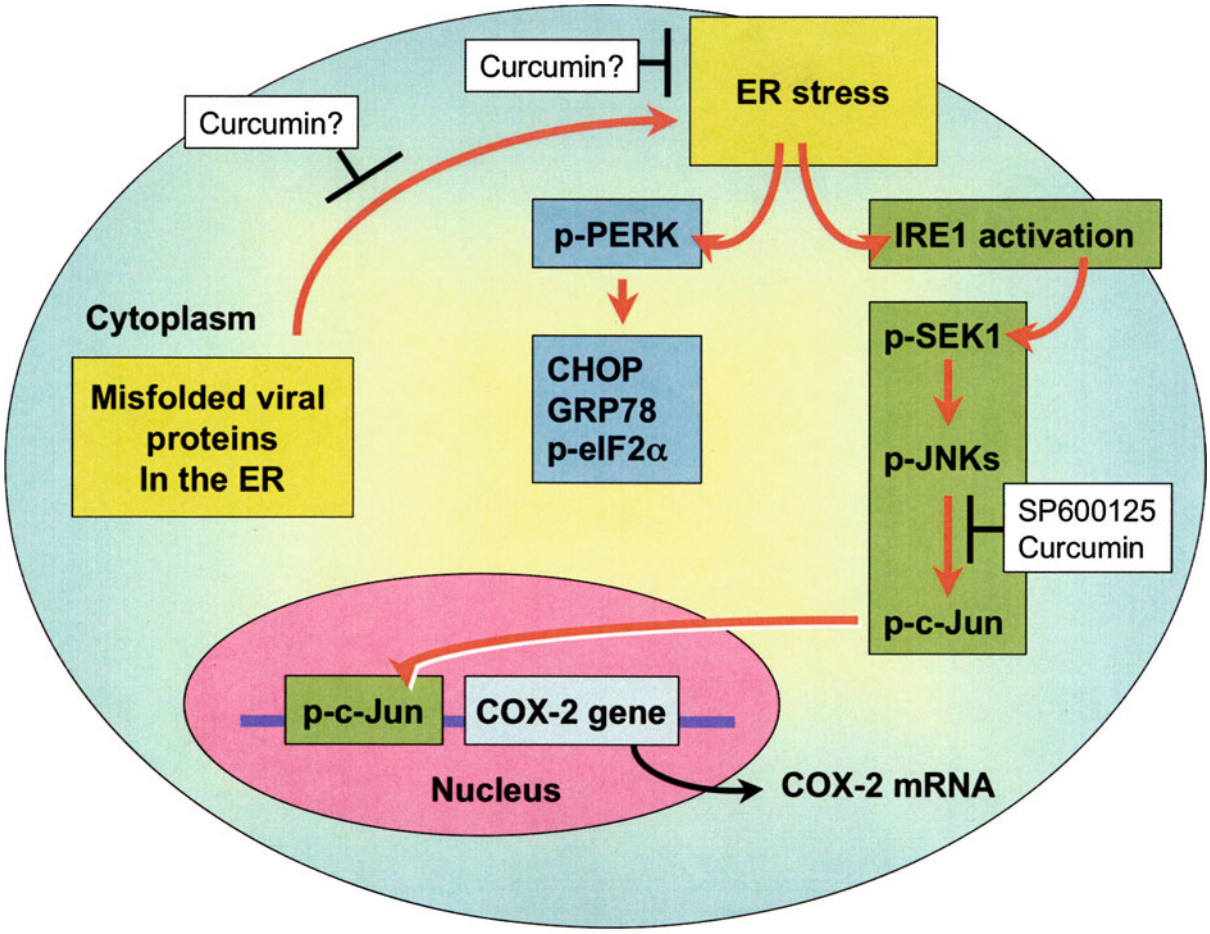

Figure 8 A hypothetical model for an ER stress–linked JNK pathway leading to up-regulation of COX-2 after *ts*1 infection in astrocytes. In this scenario, accumulation of viral envelope protein in the astrocyte ER in causes ER stress, activating ER stress signaling in which IRE1 and PERK are activated, CHOP, GRP78 and eIF2α are activated, and IRE1 activates the downstream mediators SEK1 and JNK, resulting in the phosphorylation of c-Jun, increased transcription of COX-2 mRNA, and up-regulation of COX-2 expression. Inhibition of the JNK/c-Jun signaling pathway by the JNK inhibitors curcumin and SP600125 decreases the expression of COX-2. Curcumin may also inhibit the upregulation of COX-2 by inhibiting ER stress and oxidative stress.

Materials and methods

Reagents and antibodies

Sodium orthovanadate (Na_3VO_4), sodium β-glycerophosphate, sodium fluoride (NaF), dithiothreitol (DTT), and phenylmethylsulfonyl fluoride (PMSF) were purchased from Sigma Chemical (St. Louis, MO, USA). Leupeptin, pepstatin, and aprotinin were purchased from Boehringer Mannheim (Indianapolis, IN, USA). Iodoacetamide (an isopeptidase inhibitor) was obtained from Fluka Chemical (Milwaukee, WI, USA). PD98059, SP600125, MG-132, lactacystin, ALLN, calpeptin, and curcumin (diferulolylmethane) were obtained from Calbiochem (San Diego, CA, USA). All were dissolved in dimethylsulfoxide (DMSO) or ethanol and stored at -80°C.

Antibodies recognizing phospho-specific ERK1/2, p38 kinase, JNK, c-Jun, p90RSK, SEK1, and eIF2α, and antibodies recognizing total SEK1, JNKs, and c-Jun were purchased from Cell Signaling Technologies (Beverly, MA, USA). A rabbit polyclonal antibody against COX-2 (Antibody-1) was obtained from Cayman Chemical (Ann Arbor, MI, USA). Monoclonal mouse IgG antibody against β-actin (A5441) was purchased from Sigma.

Virus

*ts*1, a temperature-sensitive mutant of MoMuLV, was propogated in the thymus–bone marrow cell line TB. Virus titers were determined using a modified direct focus-forming assay in 15F cells, which are a murine sarcoma-positive, leukemia-negative cell line, as described (Wong *et al*, 1981).

Cell culture and virus infection

Dulbecco's modified Eagle's medium (DMEM), fetal bovine serum (FBS), and other cell culture reagents

were obtained from Life Technologies (Rockville, MD, USA). The C1 astrocyte line is an immortalized murine astrocytic cell line that shows astrocyte characteristics and can be infected by *ts*1. *ts*1-infected C1 cells show cytopathic effects, stress responses, and stress defenses similar to those observed in primary astrocyte cultures infected by this virus (Lin *et al*, 1997; Liu *et al*, 2004; Qiang *et al*, 2004). For this study, C1 cells were maintained in DMEM supplemented with 10% FBS and antibiotics (100 units/ml penicillin and 100 μg/ml streptomycin). All cells were grown at 37°C in a humidified incubator containing 5% CO_2 in air. Cells were passaged biweekly and used for experiments when in the exponential growth phase.

For virus infection, C1 cells (2×10^6) were suspended in DMEM containing 1% FBS and 3 μg/ml of polybrene, and seeded in 100-mm tissue culture dishes. After culturing overnight, the medium was removed, and the cells infected with *ts*1 virus at a multiplicity of infection of 10 in DMEM containing 1% FBS and 3 μg/ml of polybrene. After 40 min of virus adsorption at 34°C under 5% CO_2, the medium was removed, and DMEM containing 5% FBS added to the culture. The plates were then incubated for varying times at 37°C (Lin *et al*, 1997). For mock infection, C1 astrocytes were prepared as described above, except that were incubated in culture medium containing polybrene, but without virus.

For studies of ERK and JNK inhibition, PD98059 (10 μM), curcumin (10, 20, and 40 μM), SP600125 (10, 20, and 40 μM), or DMSO only (control medium; <0.1%) were added to the culture medium of *ts*1-infected and mock-infected cells, and the cells were incubated for an additional 16 h before preparation of cell lysates. For studies of proteasome inhibition, MG-132 (10 μM), lactacystin (10 μM), ALLN (5 μM), or DMSO only (<0.1%) were added to the culture medium of *ts*1-infected and mock-infected cells, and the cells incubated for an additional 16 h before preparation of cell lysates, as described previously (Kim *et al*, 2001).

Animals and virus infection

FVB/N mice were obtained from Taconic Farms (Germantown, NY, USA). Mice were maintained in sterilized microisolators and supplied with autoclaved food and water *ad libitum*. Newborn FVB/N mice were inoculated intraperitoneally with 0.1 ml of *ts*1 viral suspension containing 10^7 infectious units/ml, as described previously (Stoica *et al*, 2000), whereas control mice were inoculated with medium only. The mice were then observed daily for signs of paralysis, and were killed at 25 dpi. This experimental protocol was approved by the Texas A&M University Institutional Animal Care and Use Committee.

Tissue processing

For histopathology and immunohistochemistry, *ts*1-infected ($n = 5$) and control ($n = 5$) mice were anesthetized using an intraperitoneal injection of pentobarbital (150 mg/kg) and transcardially perfused with 10% buffered formalin as a fixative using a peristaltic pump. After a 12-h fixation, each brain was dissected, with the brain segments separated for further processing. For RT-PCR and Western immunoblotting analysis of COX-2 mRNA and protein in the brainstem, *ts*1-infected ($n = 3$) and control ($n = 3$) mice were sacrificed at 25 dpi, their brains removed, and the brainstem tissues snap-frozen in liquid nitrogen and stored at −80°C.

RT-PCR analysis of COX-2 mRNA

Total RNA was isolated from brainstems of control and *ts*1-infected mice using Trizol reagent (Invitrogen, Carlsbad, CA, USA), as described previously (Kim *et al*, 2000). Briefly, 1 μg of each DNase-treated total RNA, primed with oligo (dT) primers, was retrotranscribed into cDNA in a final volume of 20 μl using the ultra HF RT-PCR system kit (Stratagene, La Jolla, CA, USA). Synthesized cDNA was amplified by a standard PCR protocol using *Taq* polymerase and primers (forward primer: 5′-GGGTTGCTGGGGGAAGAAATGTG; reverse primer 5′-GGTGGCTGTTTTGGTAGGCTGTG) specific for mouse COX-2 cDNA. To affirm the integrity of the RNA samples used in the RT-PCR reactions, parallel amplifications with oligonucleotide primers specific for mouse β-actin cDNA (forward: 5′-ATGTACGTAAGCCATCCAGGC; reverse; 5′-AAGGAAGGCTGGAAAAGAGC, yielding a 403-bp product) were performed.

A linear curve was plotted using the number of cycles of amplification (20, 25, 30, and 35 cycles) versus densitometric values of the PCR products of COX-2 and β-actin at each cycle. As linearity was obtained between 20 and 30 cycles for each of the two primer pairs, the optimal number of cycles for amplification was determined to be 25 (data not shown). Reaction products were electrophoresed on 1.5% agarose gels. Band intensities were analyzed using a densitometer (Model GS-690; Bio-Rad) equipped with the Multi-Analyst software program (Version 1.01; Bio-Rad). For quantification, the density of the COX-2 signal was normalized to that for β-actin.

Tissue and cell extracts

Brainstem tissue lysates were prepared by homogenization of frozen tissues in 10 volumes of lysis buffer containing 50 mM Tris-HCl (pH 7.9), 150 mM NaCl, 1 mM ethylenediaminetetraacetic acid (EDTA), 1 mM Na_3VO_4, 30 mM sodium β-glycerophosphate, 50 mM NaF, 10 mM iodoacetamide, 1 mM DTT, 1% Nonidet P-40, 1 mM PMSF, 10 μg/ml pepstatin, 10 μg/ml leupeptin, and 5 μg/ml aprotinin. The lysates were cleared by centrifugation at 13,000 × *g* at 4°C for 20 min, and the supernatants kept frozen at −80°C. The protein content of the lysates

was determined using the Bradford Assay (Bio-Rad, Hercules, CA, USA), with bovine serum albumin as the standard.

Western blotting
Proteins (20 to 50 μg) were separated by 6% to 12% sodium dodecyl sulfate polyacrylamide gel electrophoresis (SDS-PAGE) and then transferred to nitrocellulose membranes (Schleicher and Schuell, Keene, NH, USA). Kaleidoscope-prestained standards (Bio-Rad) were used to determine molecular weight. The membranes were incubated for 1 h in blocking buffer (20 mM Tris-HCl–buffered saline [TBS] containing 5% nonfat milk powder and 0.1% Tween 20) at room temperature, and then probed with appropriate antibodies in blocking buffer overnight at 4°C. Normal mouse or rabbit IgGs at the same dilutions were used as controls. The blots were incubated with anti-mouse or anti-rabbit IgG-peroxidase conjugates (1:1000 dilution; Kirkegaard Perry Laboratories, Gaithersburg, MD, USA), and developed using the enhanced chemiluminescence (ECL) method (Amersham Life Science, Arlington Heights, IL, USA). After imaging, the blots were stripped and reincubated with a mouse monoclonal anti-β-actin antibody to confirm equal protein loading. Densitometric analysis of autoradiographs was performed using a densitometer, as described above.

Immunohistochemistry
Paraffin-embedded sections (6 μm thick) were deparaffinized and washed with TBS for 20 min at room temperature. Potential nonspecific binding sites were blocked with 5% normal goat serum in TBS, after which the tissue sections were incubated with anti-COX-2 antibody at dilutions of 1:100 (2.0 μg/ml) for 2 h. After three 5-min washes in TBS, the sections were then incubated with biotin-conjugated secondary anti-mouse or anti-rabbit IgG (Vector Laboratories, Burlingame, CA, USA) for 30 min at room temperature. A Vecta-Elite streptavidin-peroxidase kit with a benzidine substrate was used for color development, and the sections counterstained with diluted hematoxylin. Sections that were not incubated with primary antibody served as negative controls. On these control sections, no specific immunoreactivity was detected.

Statistical analysis
Data obtained from densitometric analyses of RT-PCR and Western blots were analyzed by paired *t* test or analysis of variance (ANOVA). Additionally, statistical significance of differences between groups was determined by Dunnett's multiple comparison analysis. *P* values of $<.05$ were considered as statistically significant.

References

Alessi DR, Cuenda A, Cohen P, Dudley DT, Saltiel AR (1995). PD 98059 is a specific inhibitor of the activation of mitogen-activated protein kinase kinase in vitro and in vivo. *J Biol Chem* **270:** 27489–27494.

Almer G, Tiesmann P, Stevic Z, Halaschek-Wiener J, Deecke L, Kostic V, Przedborski S (2002). Increased levels of the pro-inflammatory prostaglandin PGE2 in CSF from ALS patients. *Neurology* **58:** 1277–1279.

Bennett BL, Sasaki DT, Murray BW, O'Leary EC, Sakata ST, Xu W, Leisten JC, Motiwala A, Pierce S, Satoh Y, Bhagwat SS, Manning AM, Anderson DW (2001). SP600125, an anthrapyrazolone inhibitor of Jun N-terminal kinase. *Proc Natl Acad Sci U S A* **98:** 13681–13686.

Chen N, Warner JL, Reiss CS (2000). NSAID treatment suppresses VSV propagation in mouse CNS. *Virology* **276:** 44–51.

Chen YR, Tan TH (1998). Inhibition of the c-Jun N-terminal kinase (JNK) signaling pathway by curcumin. *Oncogene* **17:** 173–178.

Choe W, Stoica G, Lynn W, Wong PKY (1998). Neurodegeneration induced by MoMuLV-*ts*1 and increased expression of Fas and TNF-alpha in the central nervous system. *Brain Res* **779:** 1–8.

Dimcheff DE, Askovic S, Baker AH, Johnson-Fowler C, Portis JL (2003). Endoplasmic reticulum stress is a determinant of retrovirus-induced spongiform neurodegeneration. *J Virol* **77:** 12617–12629.

Guan Z, Buckman SY, Miller BW, Springer LD, Morrison AR (1998). Interleukin-1β-induced cyclooxygenase-2 expression requires activation of both c-Jun NH_2-terminal kinase and p38 MAPK signal pathways in rat renal mesangial cells. *J Biol Chem* **273:** 28670–28676.

Han TH, Lamph WW, Prywes R (1992). Mapping of the epidermal growth factor-, serum-, and phorbol ester-responsive sequence elements in the *c-jun* promoter. Mol *Cell Biol* **12:** 4472–4477.

Hanazawa S, Takeshita A, Amano S, Semba T, Nirazuka T, Katoh H, Kitano S (1993). Tumor necrosis factor-α induces expression of monocyte chemoattractant JE via *fos* and *jun* genes in clonal osteoblastic MC3T3-E1 cells. *J Biol Chem* **268:** 9526–9532.

Harding HP, Novoa I, Zhang Y, Zeng H, Wek RC, Schapira M, Ron D (2000). Regulated translation initiation controls stress-induced gene expression in mammalian cells. *Mol Cell* **6:** 1099–1108.

Herr I, Van Dam H, Angel P (1994). Binding of promoter-associated AP-1 is not altered during induction and subsequent repression of the *c-jun* promoter by TPA and UV irradiation. *Carcinogenesis* **15:** 1105–1113.

Iwawaki T, Hosoda A, Okuda T, Kamigori Y, Nomura-Furuwatari C, Kimata Y, Tsuru A, Kohno K (2001). Translational control by the ER transmembrane kinase/ribonuclease IRE1 under ER stress. *Nat Cell Biol* **3:** 158–164.

Janelle ME, Gravel A, Gosselin J, Tremblay MJ, Flamand L (2002). Activation of monocyte cyclooxygenase-2 gene

expression by human herpesvirus 6. Role for cyclic AMP-responsive element-binding protein and activator protein-1. *J Biol Chem* **277:** 30665–30674.

Jiang Y, Chen C, Li Z, Guo W, Gegner JA, Lin S, Han J (1996). Characterization of the structure and function of a new mitogen-activated protein kinase (p38beta). *J Biol Chem* **271:** 17920–17926.

Jobin C, Bradham CA, Russo MP, Juma B, Narula AS, Brenner DA, Sartor RB (1999). Curcumin blocks cytokine-mediated NF-κB activation and proinflammatory gene expression by inhibiting inhibitory factor I-κB kinase activity. *J Immunol* **163:** 3474–3483.

Kaufman RJ (1999). Stress signaling from the lumen of the endoplasmic reticulum: coordination of gene transcriptional and translational controls. *Genes Dev* **13:** 1211–1233.

Kim HT, Qiang W, Wong PKY, Stoica G (2001). Enhanced proteolysis of IκBα and IκBβ proteins in astrocytes by Moloney murine leukemia virus (MoMuLV)-*ts*1 infection: A potential mechanism of NF-κB activation. *J NeuroVirol* **7:** 466–475.

Kim HT, Stoica G, Bazer FW, Ott TL (2000). Interferon τ-induced hepatocyte apoptosis in sheep. *Hepatology* **31:** 1275–1284.

Kitabayashi I, Saka F, Gachelin G, Yokoyama K (1990). Nucleotide sequence of the rat *c-jun* protooncogene. *Nucleic Acids Res* **18:** 3400.

Kozutsumi Y, Segal M, Normington K, Gething MJ, Sambrook J (1988). The presence of malfolded proteins in the endoplasmic reticulum signals the induction of glucose-regulated proteins. *Nature* **332:** 462–464.

Kusdra L, McGuire D, Pulliam L (2002). Changes in monocyte/macrophage neurotoxicity in the era of HAART: implications for HIV-associated dementia. *AIDS* **16:** 31–38.

Kyriakis JM, Avruch J (2001). Mammalian mitogen-activated protein kinase signal transduction pathways activated by stress and inflammation. *Physiol Rev* **81:** 807–869.

LaPointe MC, Isenovic E (1999). Interleukin-1β regulation of inducible nitric oxide synthase and cyclooxygenase-2 involves the p42/44 and p38 MAPK signaling pathways in cardiac myocytes. *Hypertension* **33:** 276–282.

Laporte JD, Moore PE, Lahiri T, Schwartzman IN, Panettieri RA Jr, Shore SA (2000). p38 MAP kinase regulates IL-1β responses in cultured airway smooth muscle cells. *Am J Physiol* **279:** L932–L941.

Lin YC, Chow CW, Yuen PH, Wong PKY (1997). Establishment and characterization of conditionally immortalized astrocytes to study their interaction with *ts*1, a neuropathogenic mutant of Moloney murine leukemia virus. *J NeuroVirol* **3:** 8–37.

Liu N, Kuang X, Kim HT, Stoica G, Qiang W, Scofield VL, Wong PKY (2004). Possible involvement of both endoplasmic reticulum- and mitochondria-dependent pathways in MoMuLV-*ts*1-induced apoptosis in astrocytes. *J NeuroVirol* **10:** 189–198.

Liu N, Quiang W, Kuang X, Thillier P, Lynn WS, Wong PKY (2002). The peroxisome proliferator phenylbutyric acid (PBA) protects astrocytes from ts1-MoMuLV-induced oxidated cell death. *J Neurovirol* **8:** 318–325.

Meriin AB, Gabai VL, Yaglom J, Shifrin VI, Sherman MY (1998). Proteasome inhibitors activate stress kinases and induce Hsp72. Diverse effects on apoptosis. *J Biol Chem* **273:** 6373–6379.

Mingetti L (2004). Cyclooxygenase-2 (COX-2) in inflammatory and degenerative brain diseases. *J Neuropathol Exp Neurol* **63:** 901–910.

Mingetti L, Walsh DT, Levi G, Perry H (1999). In vivo expression of cyclosoxygenase-2 in rat brain following intraparenchymal injection of bacterial endotoxin and inflammatory cytokines. *J Neuropathol Exp Neurol* **58:** 1184–1191.

Mohan R, Sivak J, Ashton P, Russo LA, Pham BQ, Kasahara N, Raizman MB, Fini ME (2000). Curcuminoids inhibit the angiogenic response stimulated by fibroblast growth factor-2, including expression of matrix metalloproteinase gelatinase B. *J Biol Chem* **275:** 10405–10412.

Molina-Holgado E, Ortiz S, Molina-Holgado F, Guaza C (2000). Induction of COX-2 and PGE_2 biosynthesis by IL-1β is mediated by PKC and mitogen-activated protein kinases in murine astrocytes. *Br J Pharmacol* **131:** 152–159.

Murono S, Inoue H, Tanabe T, Joab I, Yoshizaki T, Furukawa M, Pagano JS (2001). Induction of cyclooxygenase-2 by Epstein-Barr virus latent membrane protein 1 is involved in vascular endothelial growth factor production in nasopharyngeal carcinoma cells. *Proc Natl Acad Sci U S A* **98:** 6905.

Nakayama K, Furusu A, Xu Q, Konta T, Kitamura M (2001). Unexpected transcriptional induction of monocyte chemoattractant protein 1 by proteasome inhibition: involvement of the c-Jun N-terminal kinase-activator protein 1 pathway. *J Immunol* **167:** 1145–1150.

Newton R, Cambridge L, Hart LA, Stevens DA, Lindsay MA, Barnes PJ (2000). The MAP kinase inhibitors, PD098059, UO126 and SB203580, inhibit IL-1β-dependent PGE_2 release via mechanistically distinct processes. *Br J Pharmacol* **130:** 1353–1361.

Newton R, Kuitert LM, Bergmann M, Adcock IM, Barnes PJ (1997). Evidence for involvement of NF-κB in the transcriptional control of COX-2 gene expression by IL-1β. *Biochem Biophys Res Commun* **237:** 28–32.

Nishitoh H, Matsuzawa A, Tobiume K, Saegusa K, Takeda K, Inoue K, Hori S, Kakizuka A, Ichijo H (2002). ASK1 is essential for endoplasmic reticulum stress-induced neuronal cell death triggered by expanded polyglutamine repeats. *Genes Dev* **16:** 1345–1355.

Pahl HL, Baeuerle PA (1996). Activation of NF-kappa B by ER stress requires both Ca^{2+} and reactive oxygen intermediates as messengers. *FEBS Lett* **392:** 129–136.

Pasinetti GM, Aisen PS (1998). Cyclooxygenase-2 expression is increased in frontal cortex of Alzheimer's disease brain. *Neuroscience* **87:** 319–324.

Qiang W, Cahill JM, Liu J, Kuang X, Liu N, Scofield VL, Voorhees JR, Reid AJ, Yan M, Lynn WS, Wong PKY (2004). Activation of transcription factor Nrf-2 and its downstream targets in response to Moloney murine leukemia virus *ts*1-induced thiol depletion and oxidative stress in astrocytes. *J Virol* **78:** 11926–11938.

Raofi S, Wong PKY, Wilcox RE (2000). Modulation of G-protein linked cAMP accumulation in immortalized murine cortical astrocytes by retroviral infection. *Brain Res* **862:** 230–233.

Reddy ST, Wadleigh DJ, Herschmann HR (2000). Transcriptional regulation of the cycooxygenase-2 gene in activated mast cells. *J Biol Chem* **275:** 3107–3113.

Ron D, Habener JF (1992). CHOP, a novel developmentally regulated nuclear protein that dimerizes with transcription factors C/EBP and LAP and functions as a dominant-negative inhibitor of gene transcription. *Genes Dev* **6:** 439–453.

Scapagnini G, Foresti R, Calabrese V, Giuffrida Stella AM, Green CJ, Motterlini R (2002). Caffeic acid phenethyl

ester and curcumin: a novel class of heme oxygenase-1 inducers. *Mol Pharmacol* **61:** 554–561.

Seol DW, Chen Q, Zarnegar R (2000). Transcriptional activation of the hepatocyte growth factor receptor (*c-met*) gene by its ligand (hepatocyte growth factor) is mediated through AP-1. *Oncogene* **19:** 1132–1137.

Seymour ML, Gilby N, Bardin PG, Fraenkel DJ, Sanderson G, Penrose JF, Holgate ST, Johnston SL, Sampson AP (2002). Rhinovirus infection increases 5-lipoxygenase and cyclooxygenase-2 in bronchial biopsy specimens from nonatopic subjects. *J Infect Dis* **185:** 540–544.

Sharma OP (1976). Antioxidant activity of curcumin and related compounds. *Biochem Pharmacol* **25:** 1811–1812.

Shikova E, Lin YC, Saha K, Brooks BR, Wong PKY (1993). Correlation of specific virus-astrocyte interactions and cytopathic effects induced by *ts*1, a neurovirulent mutant of Moloney murine leukemia virus. *J Virol* **67:** 1137–1147.

Slice LW, Bui L, Mak C, Walsh JH (2000). Differential regulation of COX-transcription by Ras- and Rho-family of GTPases. *Biochem Biophys Res Commun* **276:** 406–410.

Stoica G, Illanes O, Tasca SI, Wong PKY (1993). Temporal central and peripheral nervous system changes induced by a paralytogenic mutant of Moloney murine leukemia virus TB. *Lab Invest* **69:** 724–735.

Stoica G, Tasca SI, Wong PKY (2000). Motor neuronal loss and neurofilament-ubiquitin alteration in MoMuLV-*ts*1 encephalopathy. *Acta Neuropathol* **99:** 238–244.

Su HL, Liao CL, Lin YL (2002). Japanese encephalitis virus infection initiates endoplasmic reticulum stress and an unfolded protein response. *J Virol* **76:** 4162–4171.

Subbaramaiah K, Chung WJ, Dannenberg AJ (1998). Ceramide regulates the transcription of cyclooxygenase-2: evidence for involvement of extracellular signal-regulated kinase/c-Jun N-terminal kinase and p38 mitogen-activated protein kinase pathways. *J Biol Chem* **273:** 32943–32949.

Subbaramaiah K, Telang N, Ramonetti JT, Araki R, DeVito B, Weksler BB, Dannenberg AJ (1996). Transcription of cyclooxygenase-2 is enhanced in transformed mammary epithelial cells. *Cancer Res* **56:** 4424–4429.

Szurek PF, Yuen PH, Ball JK, Wong PK (1990). A Val-25-to-Ile substitution in the envelope precursor polyprotein, $gPr80^{env}$, is responsible for the temperature sensitivity, inefficient processing of $gPr80^{env}$, and neurovirulence of *ts*1, a mutant of Moloney murine leukemia virus TB. *J Virol* **64:** 467–475.

Tai H, Miyaura C, Pilbeam CC, Tamura T, Ohsugi Y, Koishihara Y, Kubodera N, Kawaguchi H, Raisz LG, Suda T (1997). Transcriptional induction of cyclooxygenase-2 in osteoblasts is involved in interleukin-6-induced osteoclast formation. *Endocrinology* **138:** 2372–2379.

Teismann P, Tieu K, Choi DK, Wu DC, Naini A, Hunot S, Vila M, Jackson-Lewis V, Przedborski S (2003). Cyclooxygenase-2 is instrumental in Parkinson's disease neurodegeneration. *Proc Natl Acad Sci U S A* **100:** 5473–5478.

Tirasophon W, Welihinda AA, Kaufman RJ (1998). A stress response pathway from the endoplasmic reticulum to the nucleus requires a novel bifunctional protein kinase/endoribonuclease (Ire1p) in mammalian cells. *Genes Dev* **12:** 1812–1824.

Urano F, Wang X, Bertolotti A, Zhang Y, Chung P, Harding HP, Ron D (2000). Coupling of stress in the ER to activation of JNK protein kinases by transmembrane protein kinase IRE1. *Science* **287:** 664–666.

Wadleigh DJ, Reddy ST, Kopp E, Ghosh S, Herschman HR (2000). Transcriptional activation of the cyclooxygenase-2 gene in endotoxin-treated RAW 264.7 macrophages. *J Biol Chem* **275:** 6259–6266.

Wong PKY, Floyd E, Szurek PF (1991). High susceptibility of FVB/N mice to the paralytic disease induced by *ts*1, a mutant of Moloney murine leukemia virus TB. *Virology* **180:** 365–371.

Wong PKY, Prasad G, Hansen J, Yuen PH (1989). *ts*1, a mutant of Moloney murine leukemia virus-TB, causes both immunodeficiency and neurologic disorders in BALB/c mice. *Virology* **170:** 450–459.

Wong PKY, Soong MM, Yuen PH (1981). Replication of murine leukemia virus in heterologous cells: interaction between ecotropic and xenotropic viruses. *Virology* **109:** 366–378.

Wu HM, Wen HC, Lin WW (2002). Proteasome inhibitors stimulate interleukin-8 expression via Ras and apoptosis signal-regulating kinase-dependent extracellular signal-related kinase and c-Jun N-terminal kinase activation. *Am J Respir Cell Mol Biol* **27:** 234–243.

Xie W, Herschman HR (1996). Transcriptional regulation of prostaglandin synthase 2 gene expression by platelet-derived growth factor and serum. *J Biol Chem* **271:** 31742–31748.

Yuen PH, Szurek PF (1989). The reduced virulence of the thymotropic Moloney murine leukemia virus derivative MoMuLV-TB is mapped to 11 mutations within the U3 region of the long terminal repeat. *J Virol* **63:** 471–480.

Zhu H, Cong JP, Yu D, Bresnahan WA, Shenk TE (2002). Inhibition of cyclooxygenase 2 blocks human cytomegalovirus replication. *Proc Natl Acad Sci U S A* **99:** 3932–3937.